ARR No. 3G26

NATIONAL ADVISORY COMMITTEE FOR AERONAUTICS

WARTIME REPORT

ORIGINALLY ISSUED

July 1943 as
[redacted] Report 3G26

WORKING CHARTS FOR THE COMPUTATION OF PROPELLER THRUST THROUGHOUT THE TAKE-OFF RANGE

By Gerald L. Desmond and Robert F. Freitag
Bureau of Aeronautics, Navy Department

WASHINGTON

NATIONAL ADVISORY COMMITTEE FOR AERONAUTICS

[redacted] REPORT

WORKING CHARTS FOR THE COMPUTATION OF PROPELLER THRUST THROUGHOUT THE TAKE-OFF RANGE

By Gerald L. Desmond and Robert F. Freitag

SUMMARY

The data from NACA reports on tests conducted on full-scale propellers with 3155 blade design have been used to construct a set of propeller thrust charts for use in the calculation of take-off performance.

By use of these charts, the thrust of modern single- and dual-rotating propellers may be easily and rapidly calculated through the entire take-off range.

The thrust formula is reduced to:

$$T = \frac{K_T \ bhp}{N \ D}$$

where

T thrust in pounds

bhp brake horsepower

N propeller revolutions per minute

D propeller diameter, feet

K_T modified thrust coefficient, depending upon the ratio C_T/C_p

K_T is presented as a function of the blade activity factor times the number of blades C_p, and V/nD. Examples of the use and application of the charts are given together with calculation of the factors involved.

INTRODUCTION

An accurate evaluation of propeller thrust requires a knowledge of many variables. Empirical analyses have been developed by The Hamilton-Standard Propeller Division, United Aircraft Corporation in 1941 and by The Propeller Division, Curtiss-Wright Corporation in 1940 for deriving correction factors to account for these variables. Generally, however, these correction factors are compensating and it appears that the use of the thrust and power coefficients with a correction for solidity only is sufficient for general application in the calculation of take-off thrust and consistent with flight-test accuracy.

For the basic propeller data, the Hamilton-Standard propeller blade design No. 3155-6 has been used because the NACA has tested this blade in a wide variety of assemblies ranging from three blades to eight blades for single- and dual-rotating propellers. Also, additional tests were made with this blade section increased 50 percent in width. Thus a consistent set of propeller data covering a wide range of solidity is available. For a measure of solidity, the activity factor of the blade multiplied by the number of blades is used. This combination provides an integration of power-absorption capacity of the blade elements in addition to the propeller solidity.

It has been found convenient in making take-off calculations to plot the propeller data as a modified thrust coefficient K_T, involving engineering terms as defined by Diehl in reference 1.

It is the purpose of this report to present these data for general use.

SUMMARY OF TESTS

The data used in the construction of the thrust charts were obtained from extensive tests conducted at the NACA 20-foot propeller-research tunnel and reported in detail in references 2 to 5.

Propellers

The propeller blades tested were the 3155-6 (right hand), 3156-5 (left hand), 3155-6-1.5 (right hand), and the 3156-5-1.5 (left hand). Some additional data were incor-

porated from the tests of the 5868-9 propeller blade as presented in reference 6. The diameters were 10 feet and 9 feet for the propellers of the 3155 blade design and the 5868 blade design, respectively. Clark-Y blade sections were employed throughout.

Body

The propellers were tested on a test rig consisting of a streamline body with provisions for mounting the propellers in both the tractor and the pusher positions. In the charts presented herein, only the data from the tests on the propellers in the tractor position are used. These data include the effect of a symmetrical wing mounted in a midwing position set at 0° angle of attack. Spinners were used for all tests.

SYMBOLS

$C_P = \frac{P}{\rho n^3 D^5}$, power coefficient

$C_T = \frac{T}{\rho n^2 D^4}$, thrust coefficient

$J = V/nD$, advance-diameter ratio

P engine power, foot-pounds per second

T propeller thrust in pounds

N rotational propeller speed, rpm

n rotational propeller speed, rps

D propeller diameter, feet

V airspeed, feet per second

ρ mass density of air, slugs/ft^3

K_T modified thrust coefficient, $33{,}000 \frac{C_T}{C_P}$

K_{T_o} modified static thrust coefficient

AF activity factor $= \frac{100000}{16} \int_{0.2}^{1.0} \left(\frac{b}{D}\right)\left(\frac{r}{R}\right)^3 d\left(\frac{r}{R}\right)$

b propeller blade width at radius r

r radius of propeller blade element

R propeller radius

METHOD OF PRESENTATION

Curves of K_T against AF times the number of blades with varying values of C_P and J are presented in figures 1 to 5 for single-rotating propellers and in figures 11 to 15 for dual-rotating propellers. Curves of K_T against C_P with varying values of J and AF times the number of blades and curves of K_T against J with varying values of C_P and AF times the number of blades are presented in figures 6 to 10 for single-rotating propellers and in figures 16 to 20 for dual-rotating propellers.

From references 2 to 5 values of C_P and C_T for the various blade angles tested were obtained for each propeller and the thrust coefficients K_T were computed. The available data consisted of curves of C_T and C_P against V/nD for blade angles of 10° to 65°.

The propellers were tested at values of J as low as 0.3 and, in a few cases, to values as low as J = 0.2. The necessity then arose to extrapolate the curves C_P and C_T to the value of V/nD = 0, in order to obtain static thrust coefficients. In a small number of cases, extrapolations made by the NACA were included in the original data. These extrapolations, when available, were followed. Later, calculated curves of C_P and C_T against J were presented by the NACA wind-tunnel staff in an unpublished report. These calculated curves were found to be in excellent agreement with the test data throughout the ranges in which they could be compared. It was then concluded that extrapolations of the test data, based on these computed curves, could be used. These extrapolations were most accurate at low-blade angles and low-power coefficients. It is under these conditions that the propeller is operating near the maximum value of L/D. At the higher blade angles

and power coefficients, the variation of K_T with J is small, and small errors in the extrapolations will not materially offset the fairings.

Recent unpublished data presenting outdoor static-thrust tests of the 3155-6 and 3155-6-1.5 blades show excellent agreement with the static thrust data as presented in this report.

Thrust Calculation

The calculation of the thrust is simply performed. The activity factor of the blade is obtained from the geometric characteristics of the blade. Curves of activity factor of a blade against propeller diameter for a large number of propeller blades now in use are presented in figures 21 to 24. The power coefficient C_p is computed from the engine and propeller characteristics. For a constant-speed propeller, this value of C_p will remain constant throughout the take-off range. For a fixed-pitch propeller, the value of C_p will vary with airspeed which necessitates additional calculations. In this case, a method similar to that outlined in reference 6 should be used. The value of the advance ratio V/nD is computed at the various speeds during take-off for which the thrust is desired. The value of K_T is then read from the charts or by interpolation between the charts. This is most easily performed by reading figures 1 to 5 (or 11 to 15) and using figures 6 to 10 (or 16 to 20) to facilitate interpolation.

The thrust is then computed from the formula

$$T = \frac{K_T \text{ bhp}}{N D}$$

The data from which these charts were derived were obtained in tests at relatively low propeller tip speeds. Inasmuch as these charts were designed for a quick evaluation of the thrust during take-off, and the take-off distance in turn is primarily affected by airplane drag, lift coefficient at take-off, and handling technique in addition to the propeller thrust, it is assumed that changes of thrust due to propeller tip speed are of secondary order in take-off evaluation up to a tip speed of 1000 feet per second at sea level. In order to avoid excessive losses in propeller efficiency due to compressi-

bility at high speeds at altitude, take-off tip speeds greater than 1000 feet per second are not generally encountered.

Example

Given: Propeller - constant-speed, single rotation
12 ft 0 in.
three blades
blade design 6235
AF = 100
AF × number of blades = 300

Engine 2000 bhp
2700 engine rpm
2:1 reduction gear

The data may be conveniently tabulated as follows:

V	V/nD	C_p	AF × number of blades	K_T	T
0	0.0000	0.1631	300	40,000	4935
25	.0925	.1631	300	39,000	4810
50	.1850	.1631	300	38,000	4690
75	.2775	.1631	300	37,000	4565
100	.3700	.1631	300	36,000	4440

To interpolate between charts, for example, at V = 100 feet per second (J = 0.3700), the following method is most satisfactory.

Referring to figure 3, at AF × number of blades = 300, C_p = 0.1631, and J = 0.40, we find K_T = 35,500.

Selecting the plot of K_T against J for the value of AF × number of blades nearest to that being used (fig. 7), at J = 0.40 at K_T = 35,500, use the slope of the nearest C_p line to pass to J = 0.370. Then K_T = 36,000.

$$\text{Thrust} = \frac{K_T \text{ bhp}}{N\ D} = 4445 \text{ pounds}$$

To find the thrust at V = 25 feet per second (J = 0.0925):

Referring to figure 2, at AF × number of blades = 300, C_p = 0.1631, J = 0.300, we find K_T = 36,600.

Entering figure 7 at J = 0.300 and K_T = 36,600, we use the slope of the nearest C_p line to pass to J = 0.0925. Then K_T = 39,000.

$$\text{Thrust} = \frac{K_T \text{ bhp}}{N D} = 4810 \text{ pounds}$$

DISCUSSION

The use of the activity factor as a parameter for representing solidity is considered desirable as this factor is a weighted measure of propeller solidity. The activity factor of the blade is a nondimensional function of the propeller plan form designed to express the integrated capacity of the blade elements for absorbing power. In a propeller the velocity of the air passing over the blade element, and therefore its power absorption, is mainly a function of the distance of the element from the center of rotation. This fact was not allowed for in the older form of blade-area function, the ratio of blade area to total disk area. The activity factor of the whole propeller is equal to the activity factor of the blade multiplied by the number of blades.

The high activity factors of the propellers were obtained by increasing the number of blades and by increasing the blade width. Although these two methods are not strictly comparable as a means of increasing the solidity of a propeller, excellent agreement was found throughout the regions that the two methods coincided. This is in agreement with reference 4, which concludes that increasing the solidity by means of increasing the blade width results in the same effect as increasing the number of blades. Increasing the blade area by increasing the diameter had about the same effect as increasing the solidity, for equal tip speeds.

The plots represent a complete family of propellers of the 3155 blade design, from two to eight blades. The inclusion of the 5868-9 blade-design propeller data of reference 6 aided in the generalization of the charts and

facilitated the fairing of the curves in the region of low solidity.

The agreement between the 5868-9 propeller data (reference 6) and the 3155 propeller data (references 2 to 5) was, in general, quite good. Wherever small discrepancies did occur, the more recent 3155 propeller data were favored in view of the later design of this blade.

The use of Clark-Y airfoil sections throughout the analysis further standardizes the curves.

Bureau of Aeronautics, Navy Department,
Washington, D. C.

REFERENCES

1. Diehl, Walter S.: Static Thrust of Airplane Propellers. Rep. No. 447, NACA, 1932.

2. Biermann, David, and Hartman, Edwin P.: Wind-Tunnel Tests of Four- and Six-Blade, Single- and Dual-Rotating Tractor Propellers. Rep. No. 747, NACA, 1942.

3. Biermann, David, and Gray, W. H.: Wind-Tunnel Tests of Eight-Blade Single- and Dual-Rotating Propellers in the Tractor Position. NACA A.R.R., Nov. 1941.

4. Biermann, David, Gray, W. H., and Maynard, Julian D.: Wind-Tunnel Tests of Single- and Dual-Rotating Tractor Propellers of Large Blade Width. NACA A.R.R., Sept. 1942.

5. Gray, W. H.: Wind-Tunnel Tests of Single- and Dual-Rotating Tractor Propellers at Low Blade Angles and of Two- and Three-Blade Tractor Propellers at Blade Angles up to 65°. NACA A.R.R., Feb. 1942.

6. Hartman, Edwin P., and Biermann, David: The Aerodynamic Characteristics of Full-Scale Propellers Having 2, 3, and 4 Blades of Clark-Y and R.A.F. 6 Airfoil Sections, Rep. No. 640, NACA, 1938.

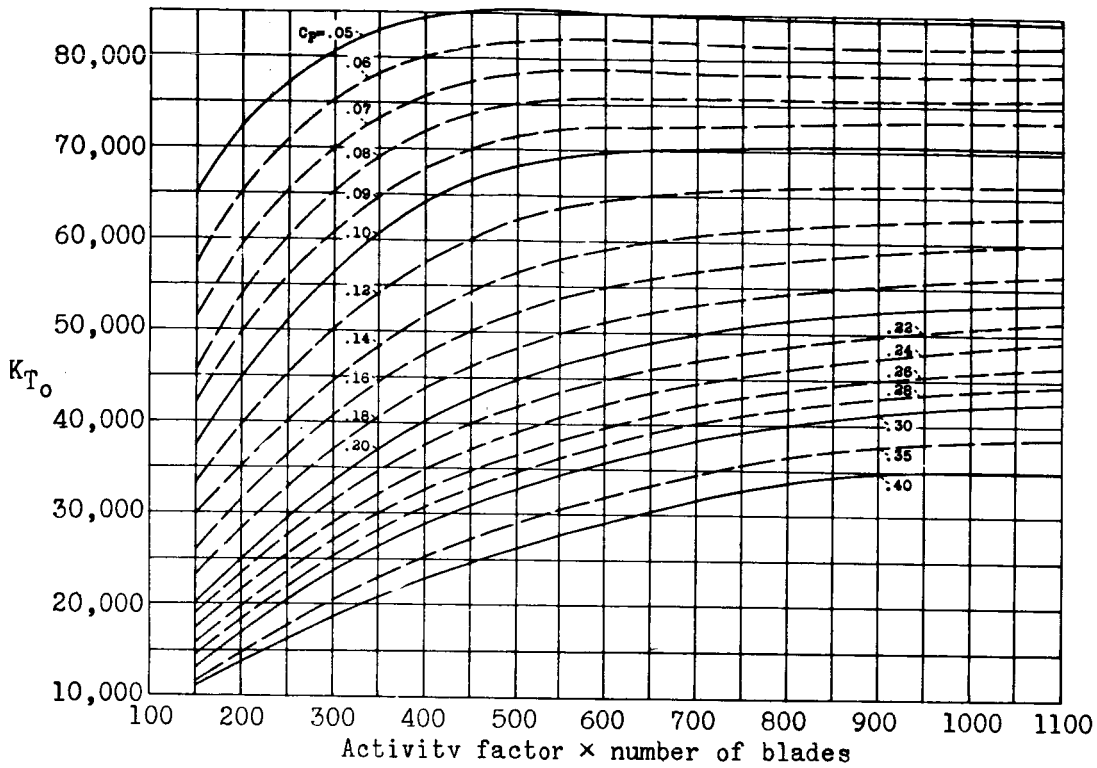

Figure 1.- Variation of K_{T_o} with solidity. 3155 propeller III single rotation. V/nD = 0, J = 0.

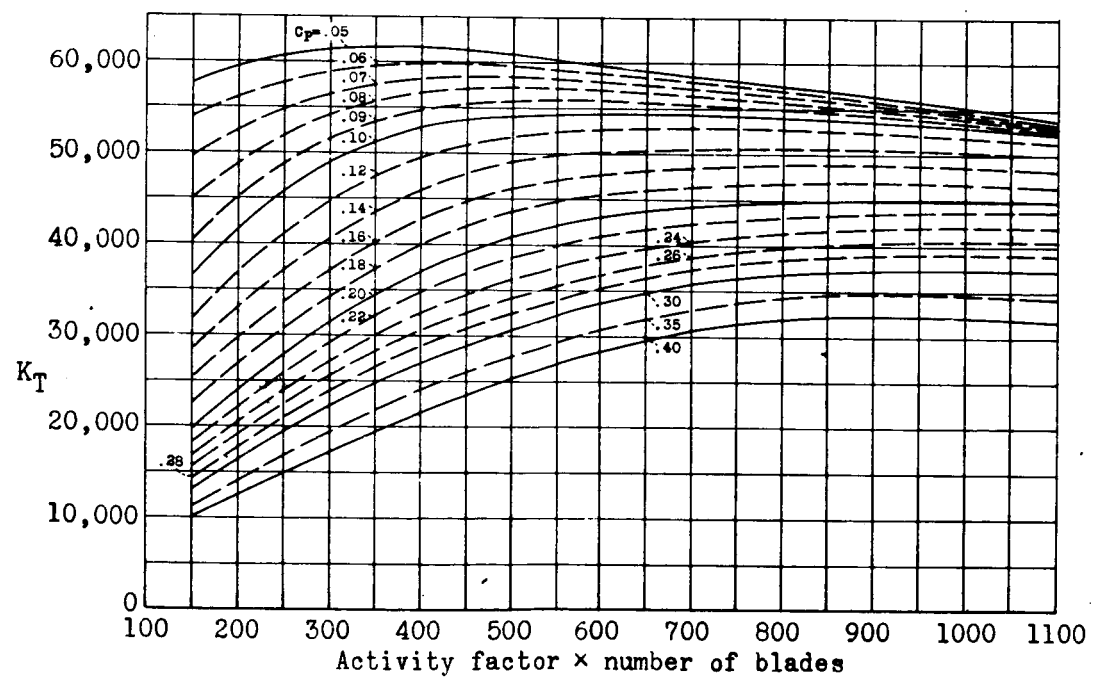

Figure 2.- Variation of K_T with solidity. 3155 propeller III single rotation. V/nD = 0.3, J = 0.3.

(1 block = 10 divisions on 1/40" Engr. scale)

W-100

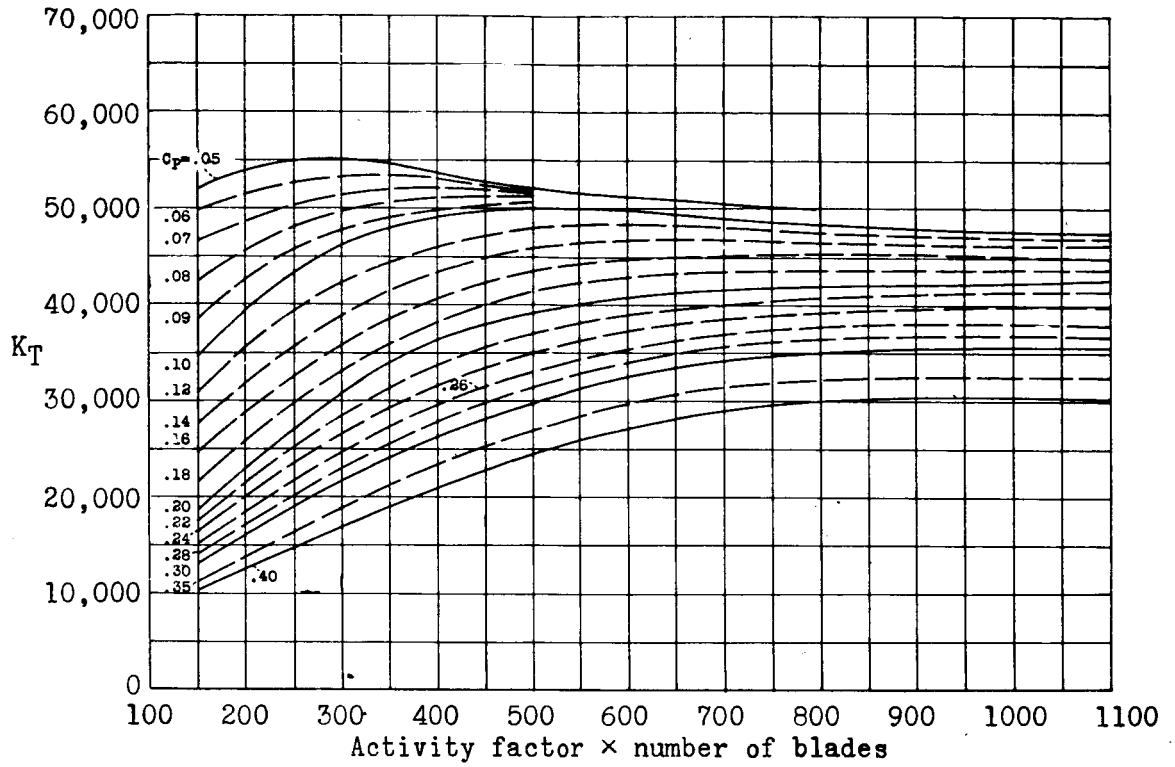

Figure 3.- Variation of K_T with solidity. 3155 propeller III single rotation. V/nD = 0.4, J = 0.4.

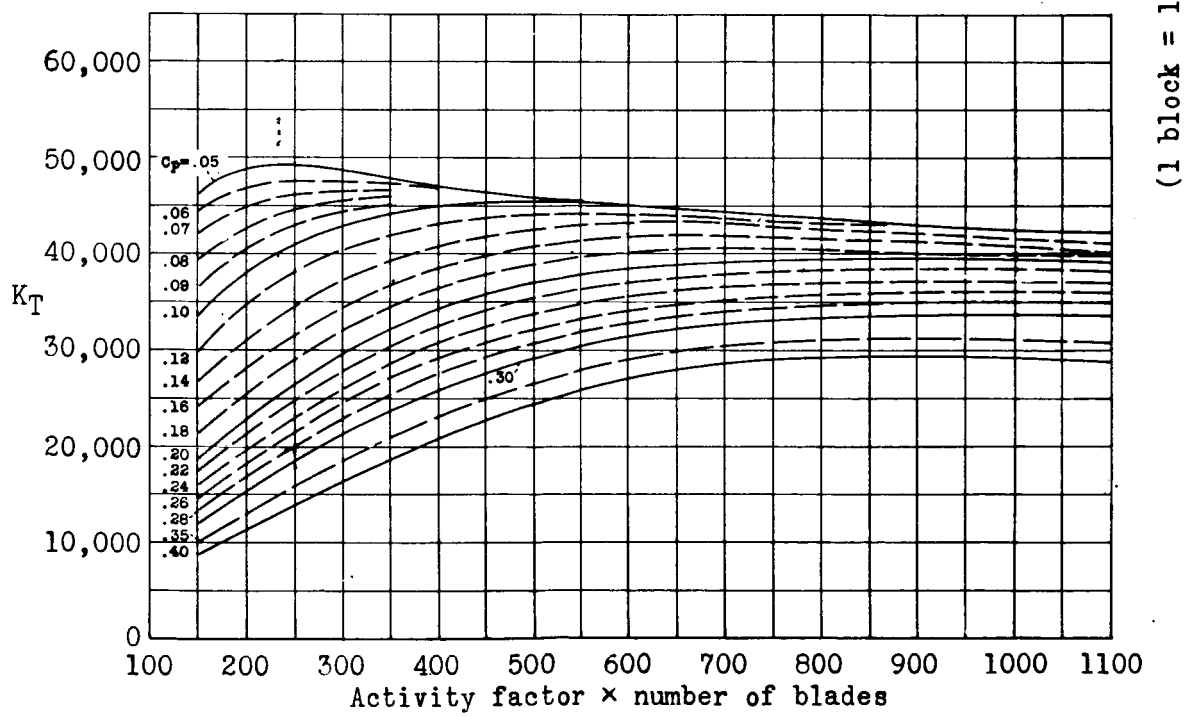

(1 block = 10/40")

Figure 4.- Variation of K_T with solidity. 3155 propeller III single rotation. V/nD = 0.5, J = 0.5.

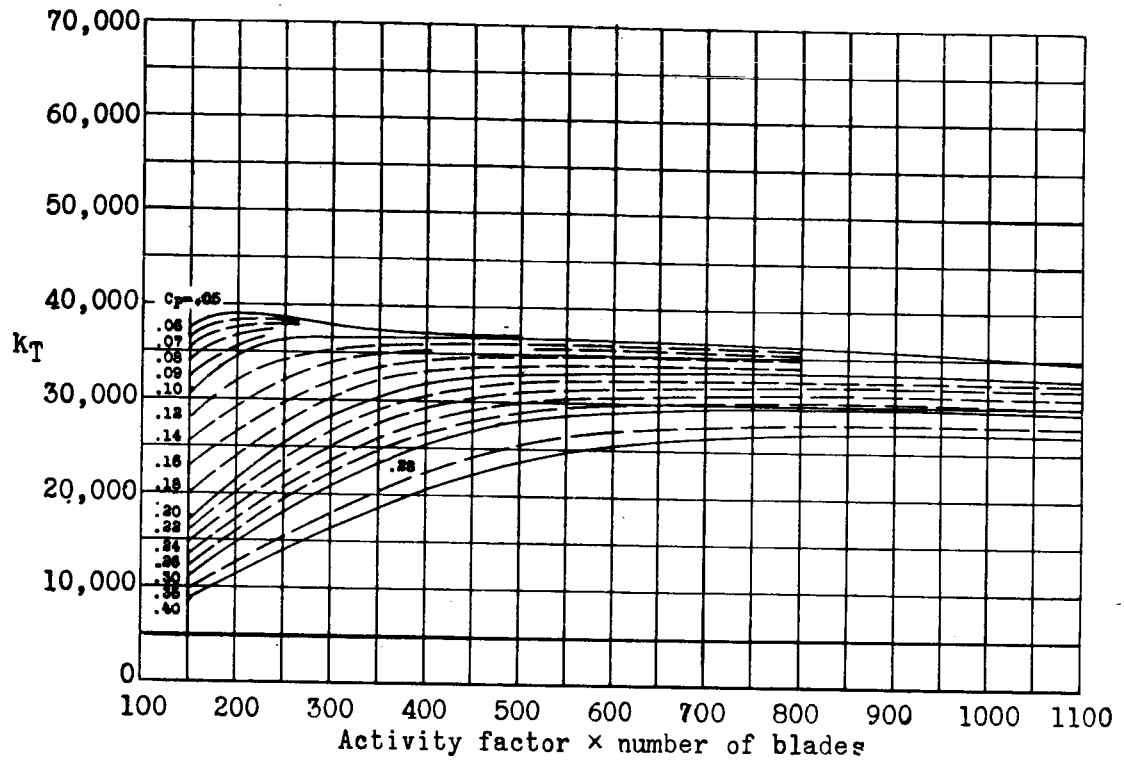

Figure 5.- Variation of K_T with solidity. 3155 propeller III single rotation. V/nD = 0.7, J = 0.7.

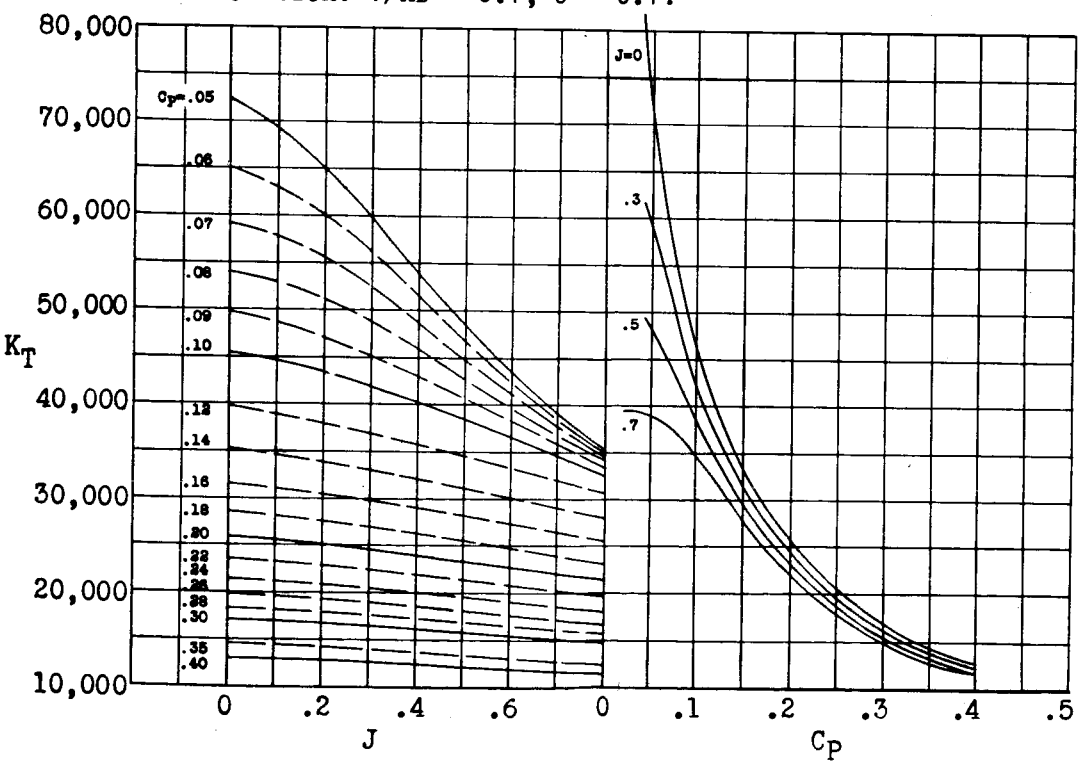

Figure 6.- 3155 propeller III single rotation. AF × number of blades = 200.

(1 block = 10/40")

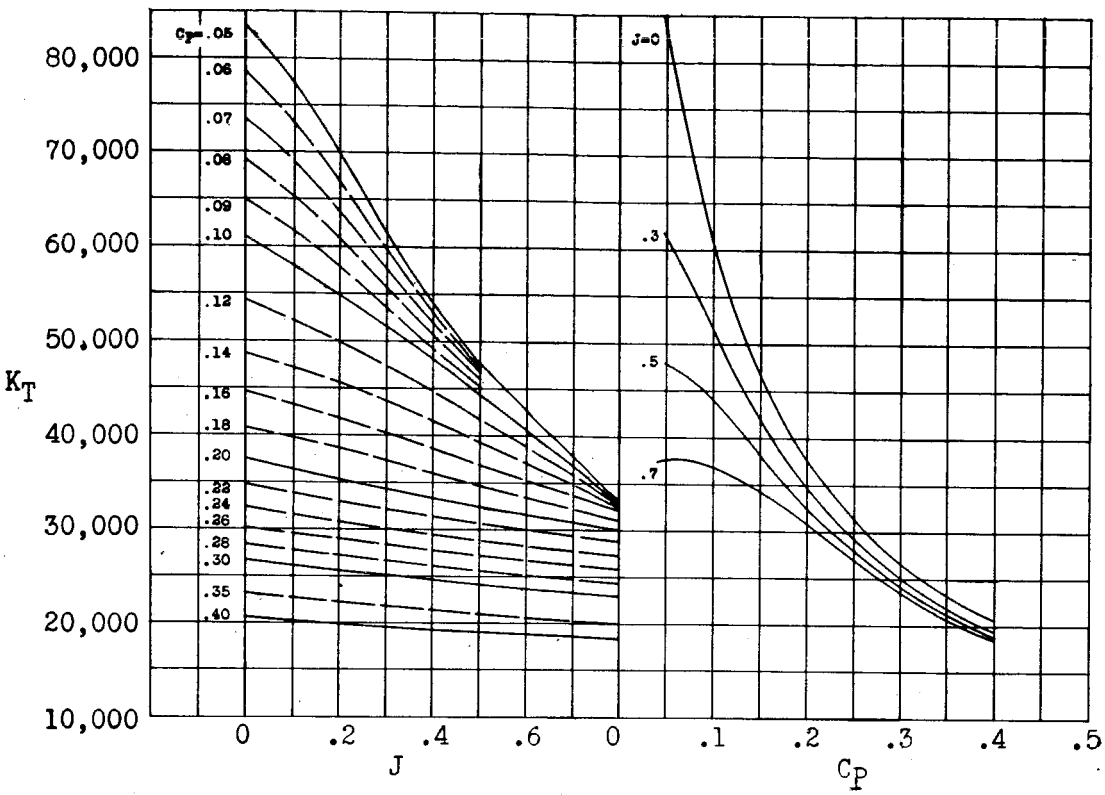

Figure 7.- 3155 propeller III single rotation. AF × number of blades = 350.

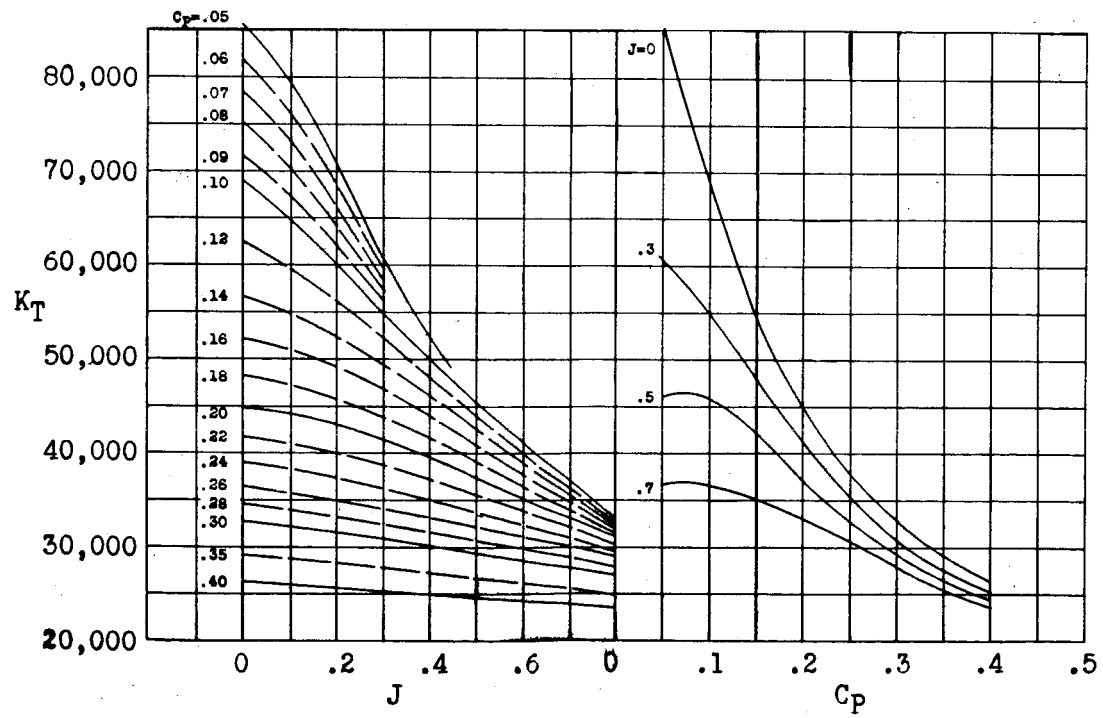

Figure 8.- 3155 propeller III single rotation. AF × number of blades = 500.

(1 block = 10/40")

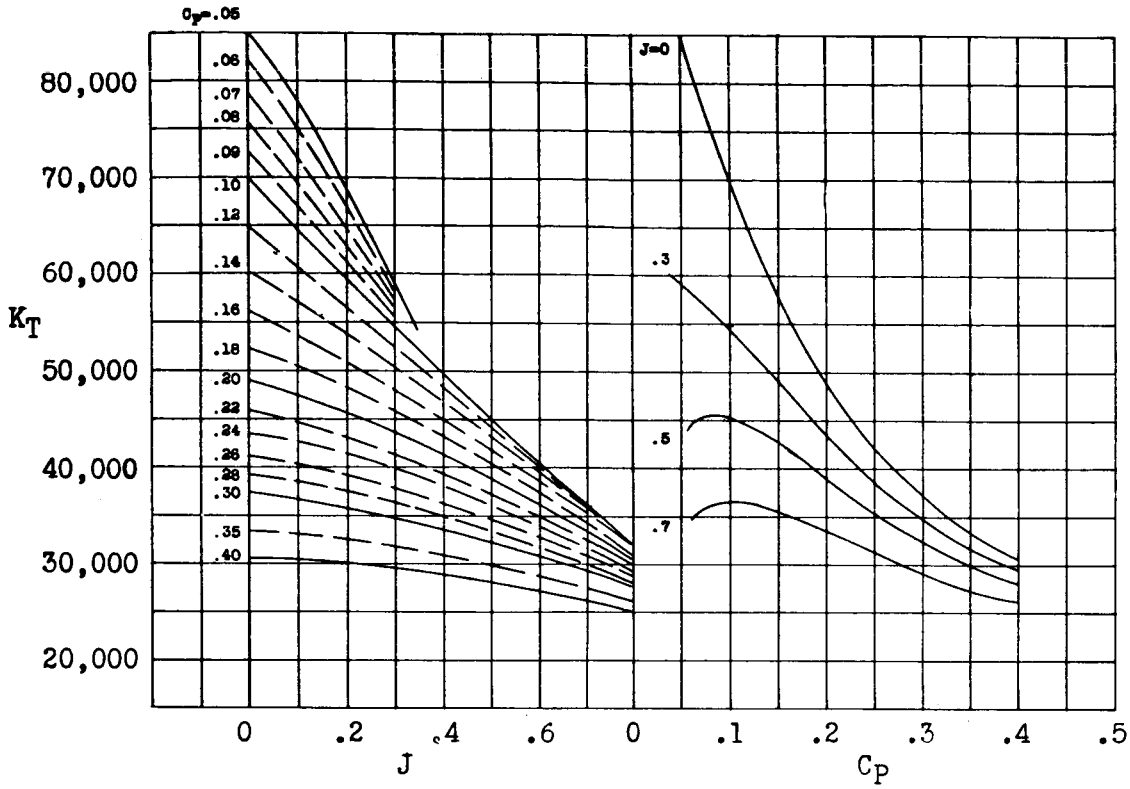

Figure 9.- 3155 propeller III single rotation. AF × number of blades = 650.

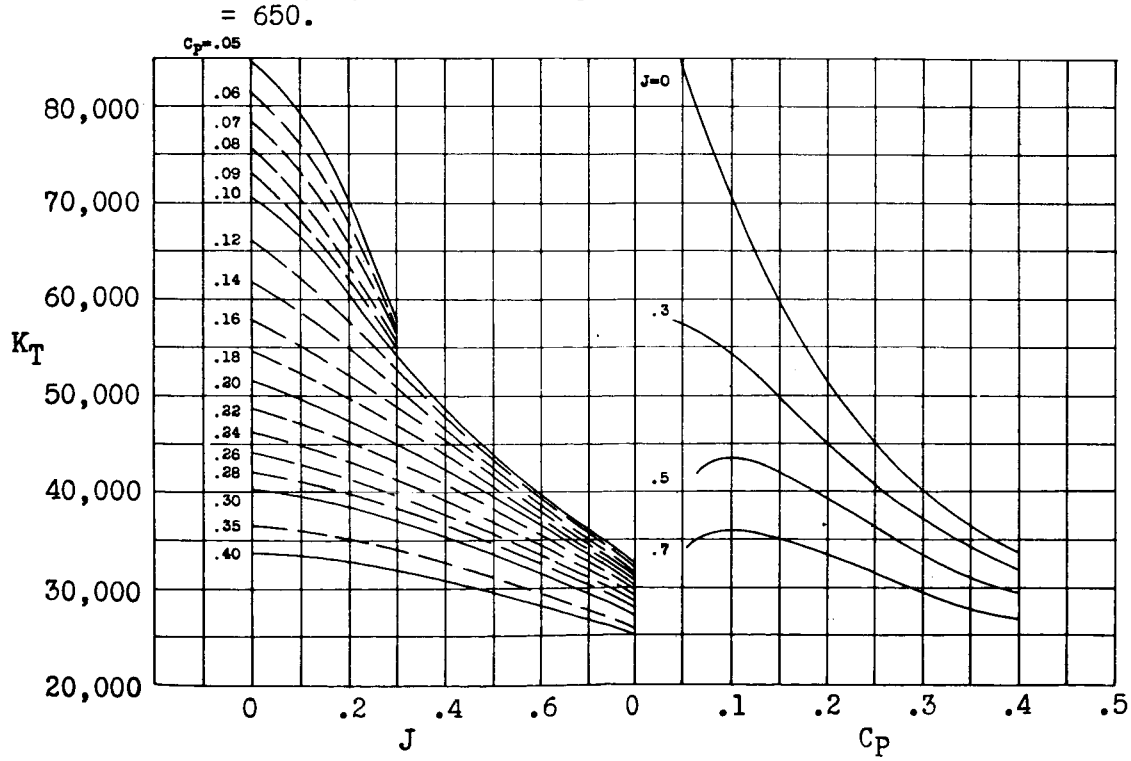

Figure 10.- 3155 propeller III single rotation. AF × number of blades = 800.

(1 block = 10/40")

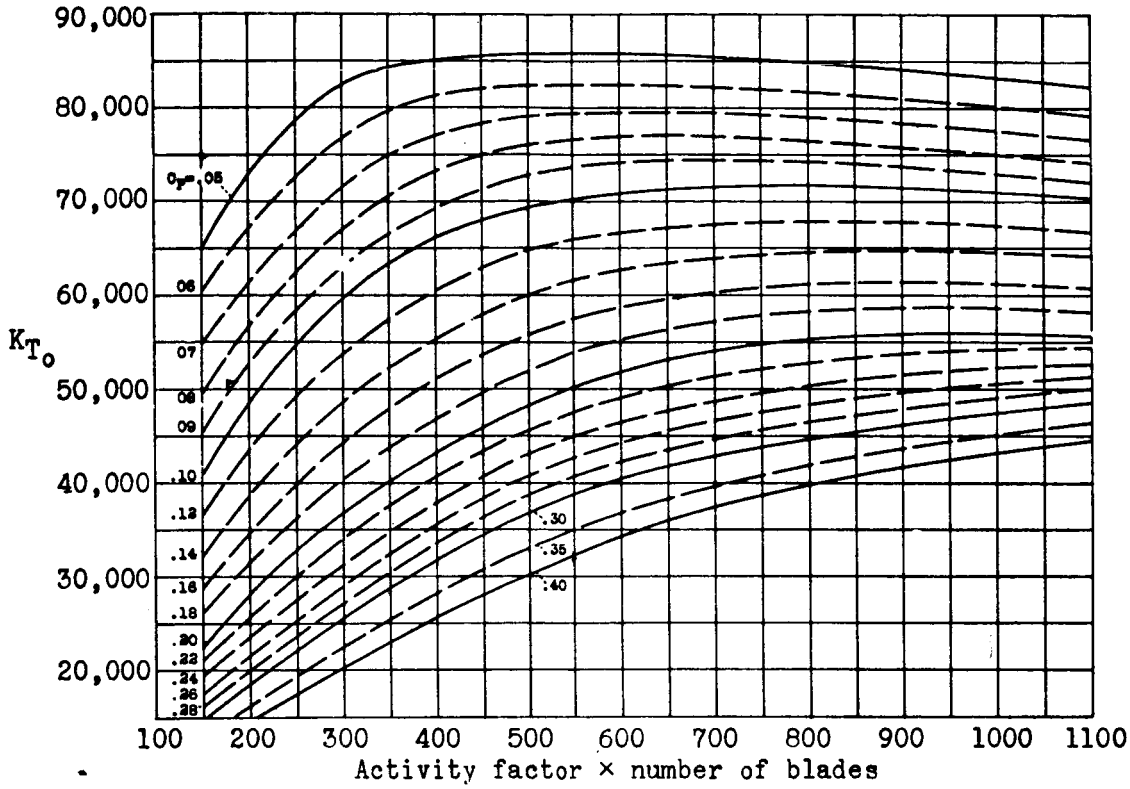

Figure 11.- Variation of K_{T_o} with solidity. 3155 propeller III static thrust dual rotation. V/nD = 0, J = 0.

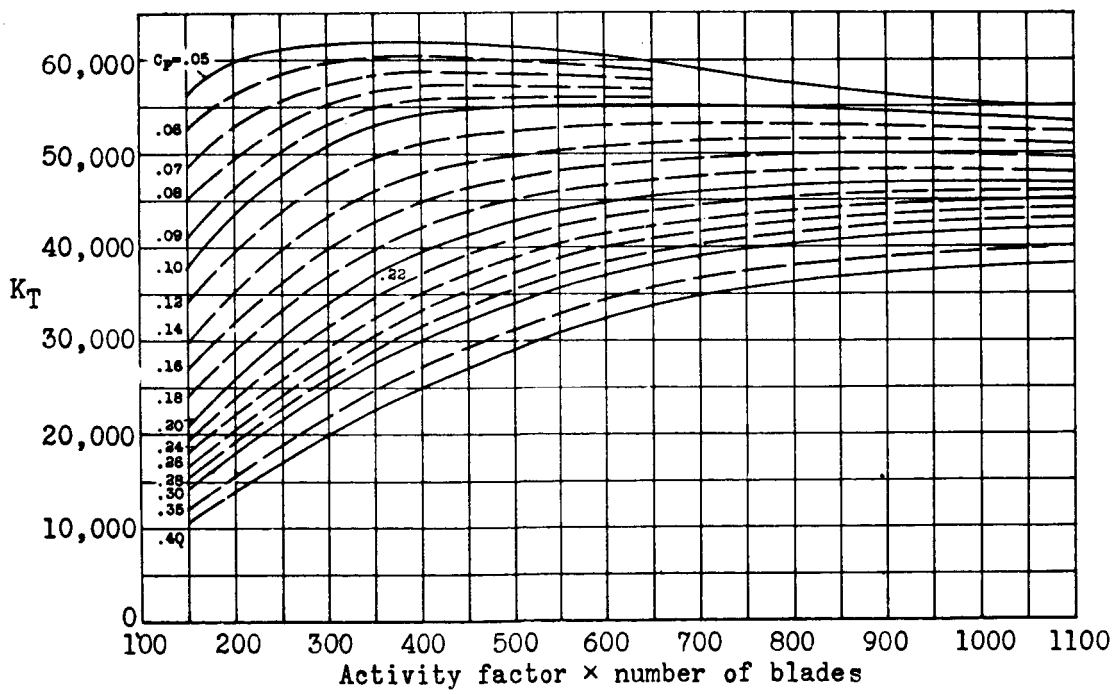

Figure 12.- Variation of K_T with solidity. 3155 propeller III dual rotation. V/nD = 0.3, J = 0.3.

(1 block = 10/40")

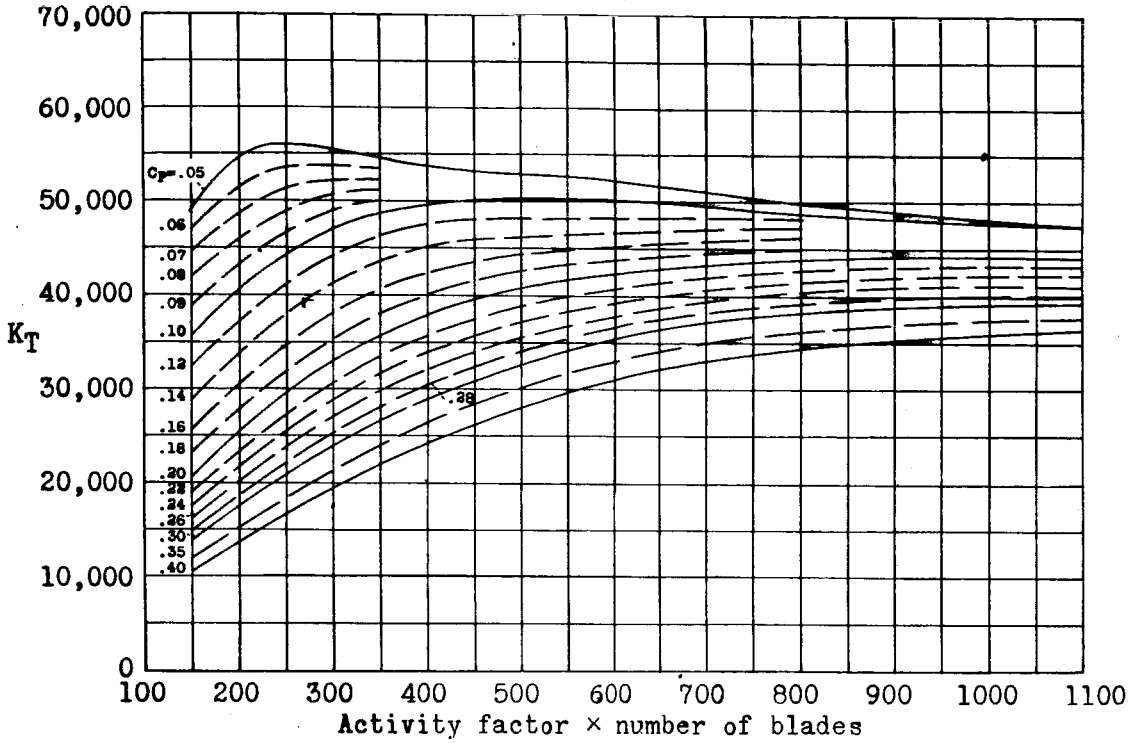

Figure 13.- Variation of K_T with solidity. 3155 propeller III dual rotation. V/nD = 0.4, J = 0.4

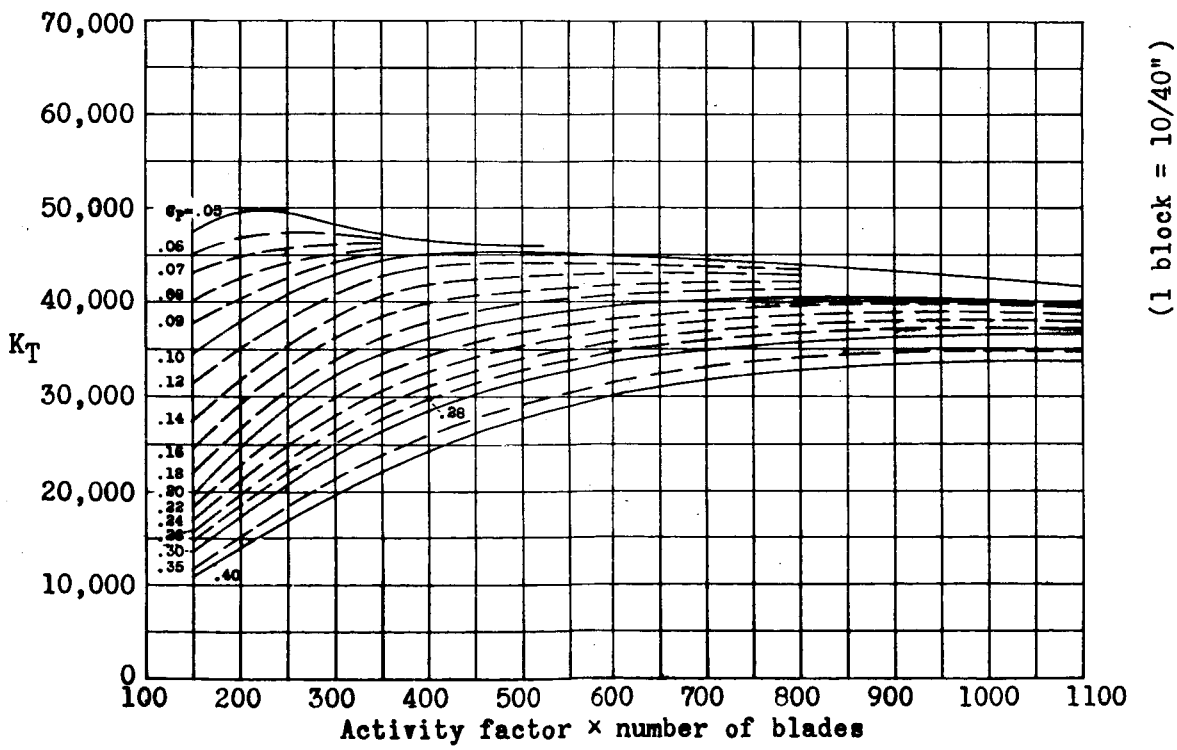

Figure 14.- Variation of K_T with solidity. 3155 propeller III dual rotation. V/nD = 0.5, J = 0.5.

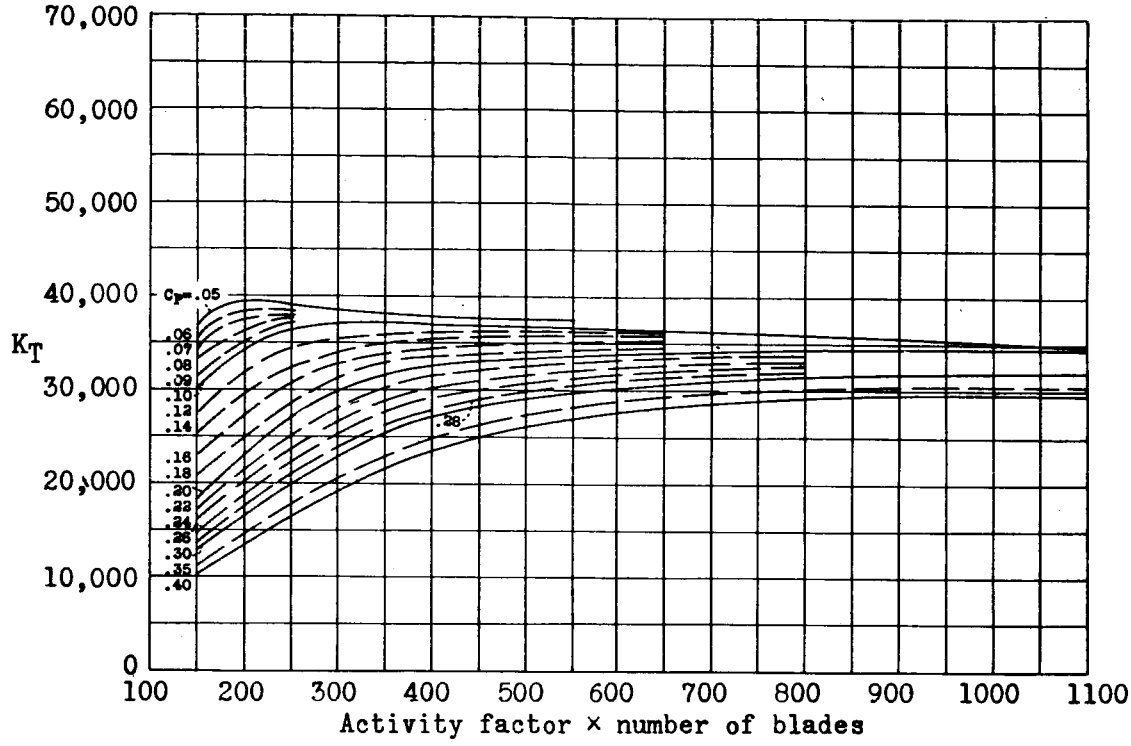

Figure 15.- Variation of K_T with solidity. 3155 propeller III dual rotation. V/nD = 0.7, J = 0.7.

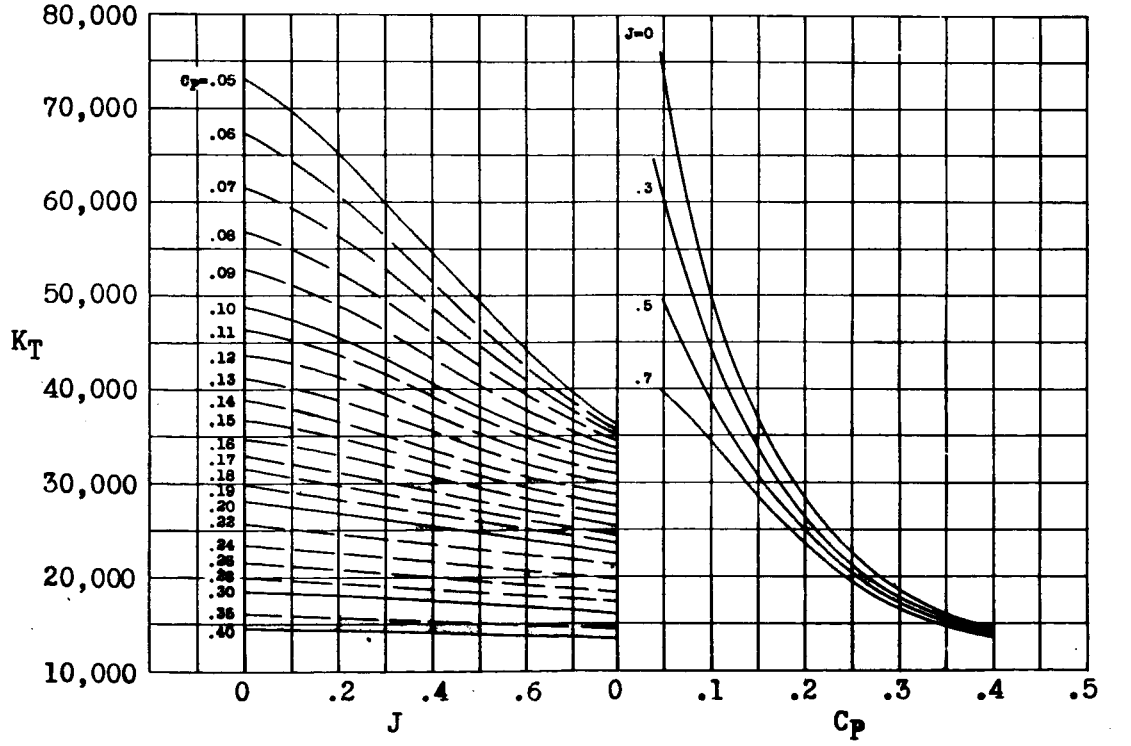

Figure 16.- Thrust coefficient against J and Cp. 3155 propeller III dual rotation. AF × number of blades = 200.

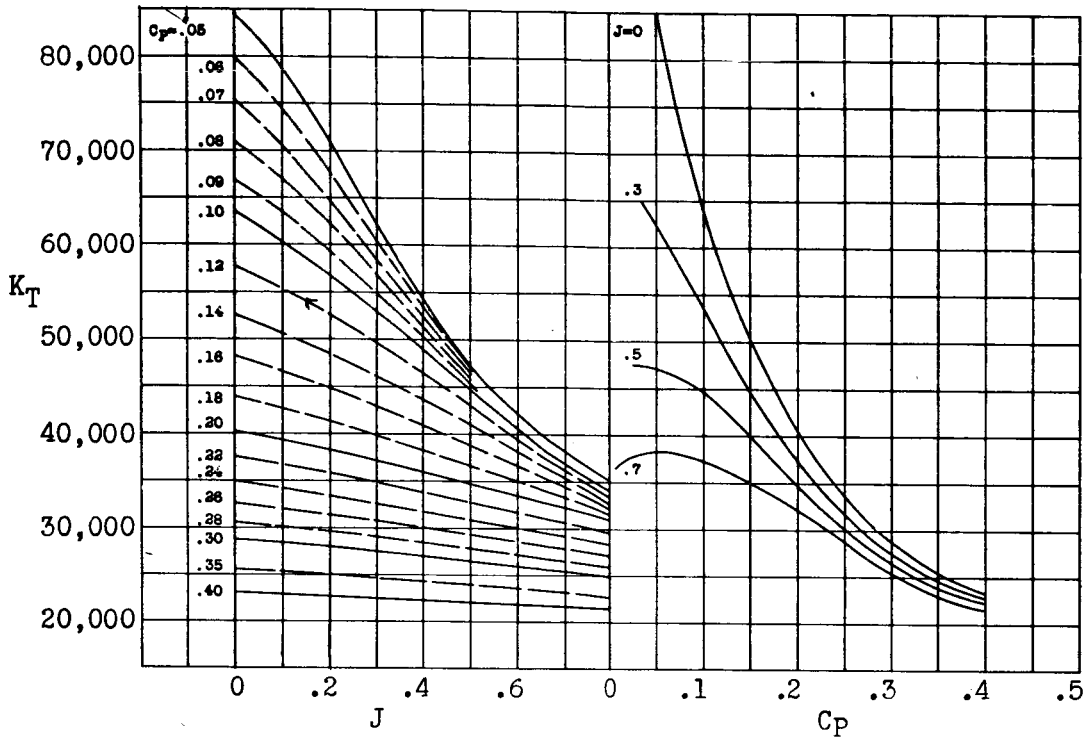

Figure 17.- 3155 propeller III dual rotation. AF × number of blades = 350.

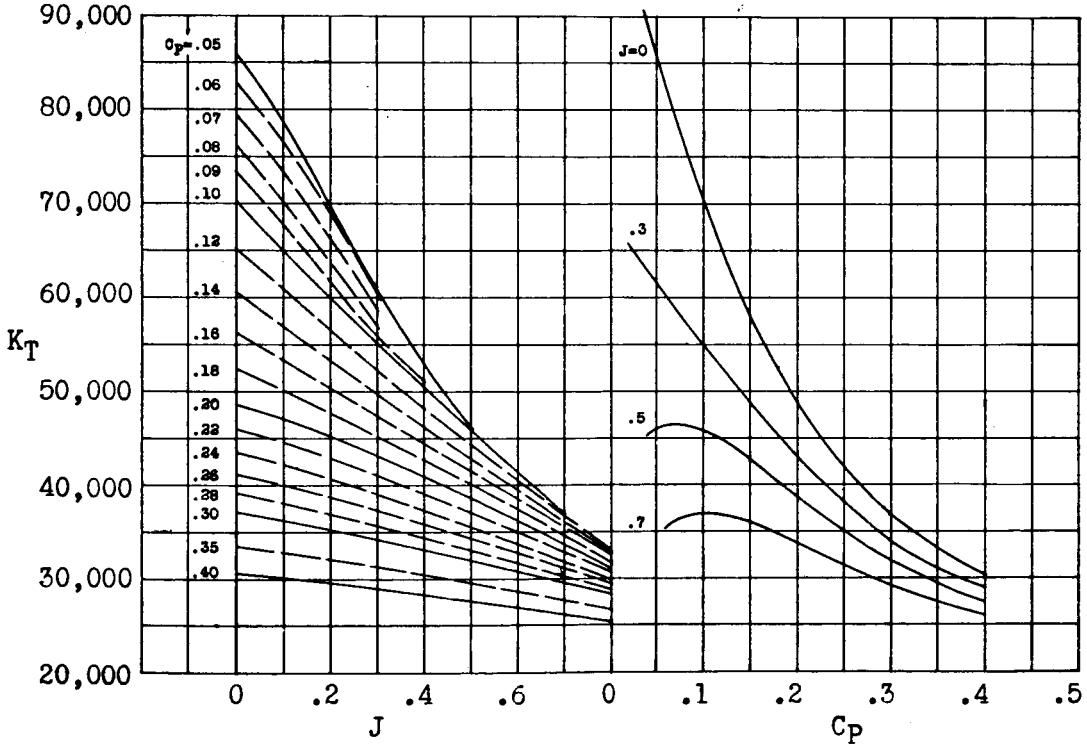

Figure 18.- 3155 propeller III dual rotation. AF × number of blades = 500.

(1 block = 10/40")

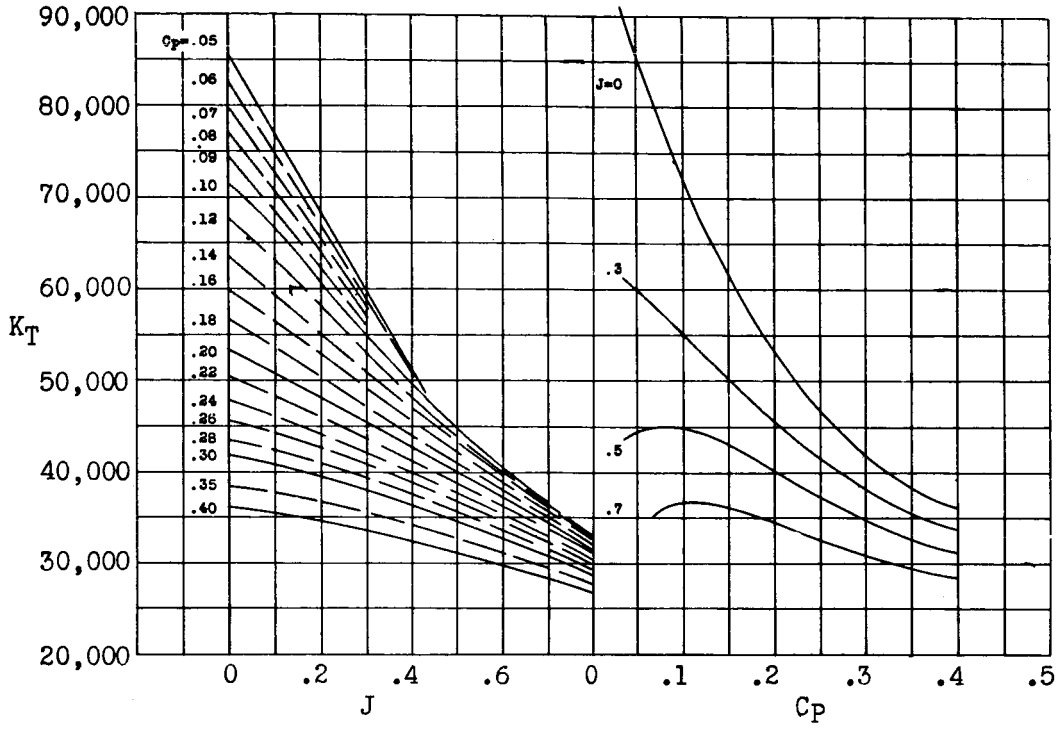

Figure 19.- 3155 propeller III dual rotation. AF × number of blades = 650.

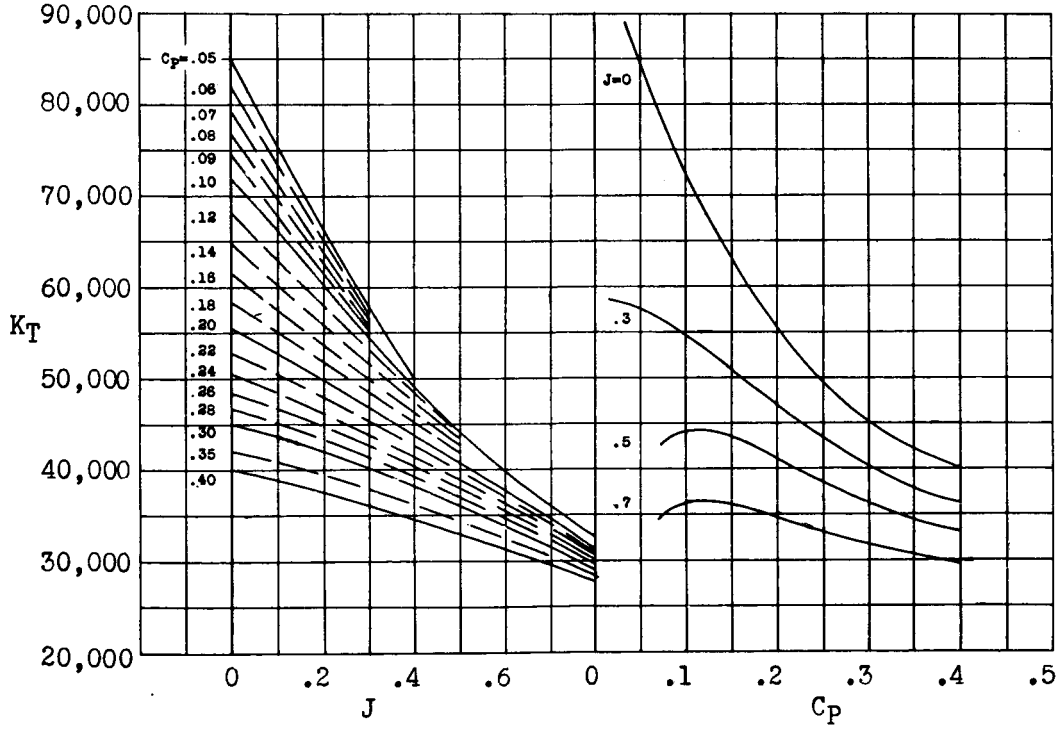

Figure 20.- 3155 propeller III dual rotation. AF × number of blades = 800.

(1 block = 10/40")

W-100

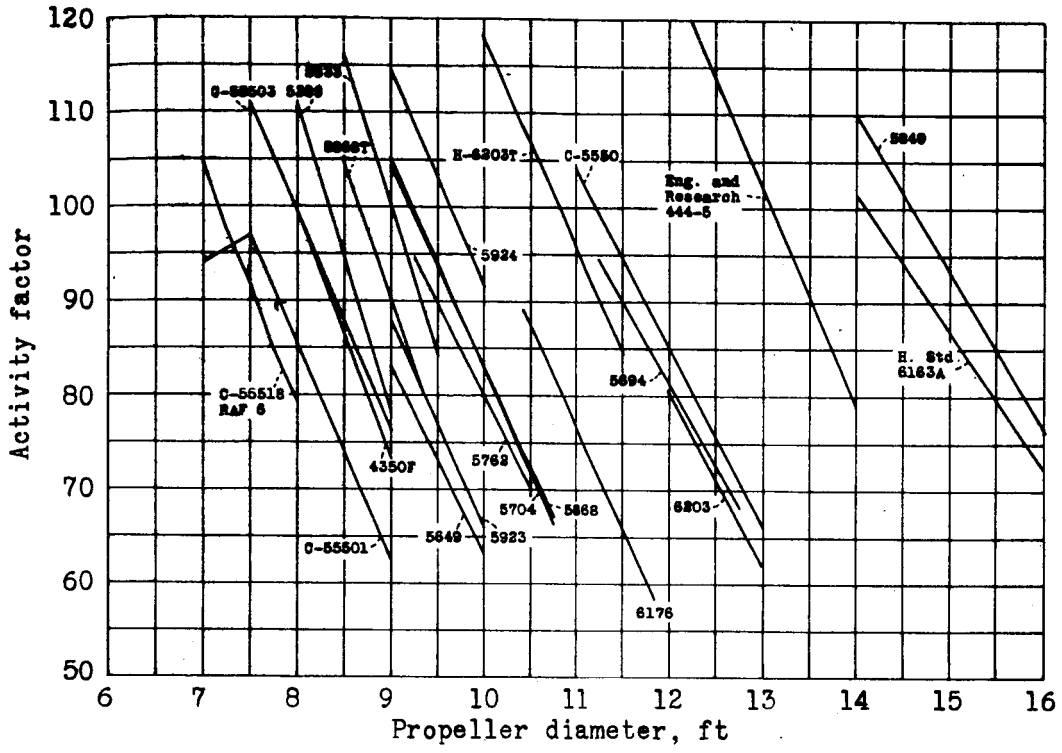

Figure 21.- Activity factors for various propellers. C = Curtiss, H = Hamilton Standard.

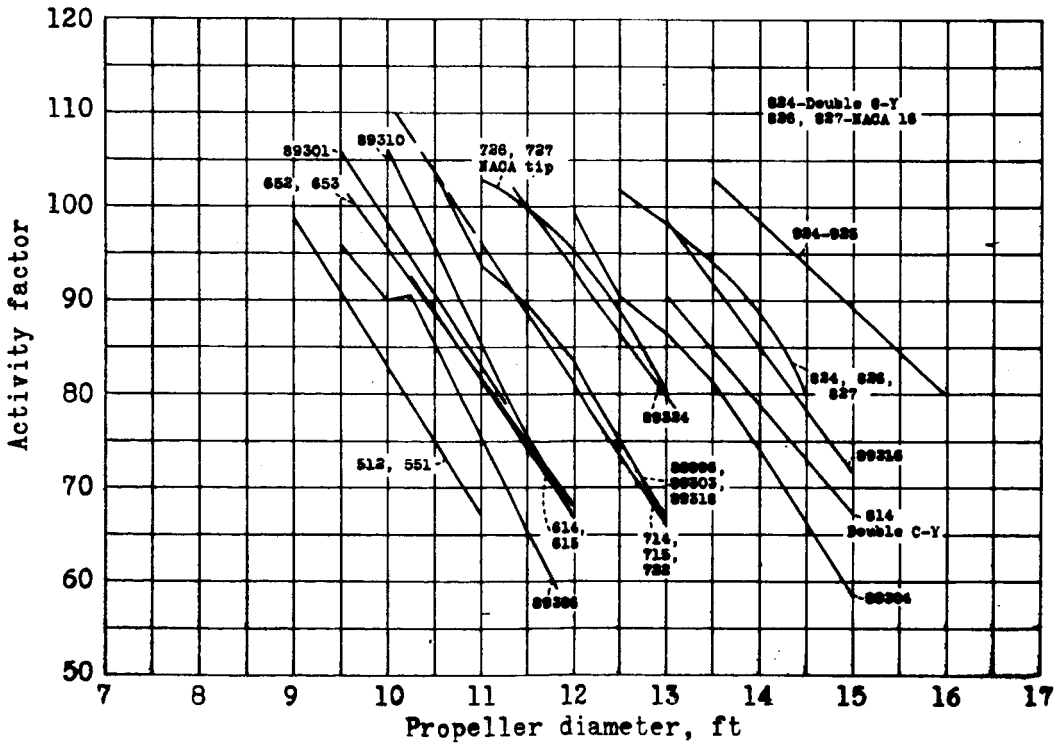

Figure 22.- Activity factors for various Curtiss propellers. Clark-Y except as noted.

(1 block = 10/40")

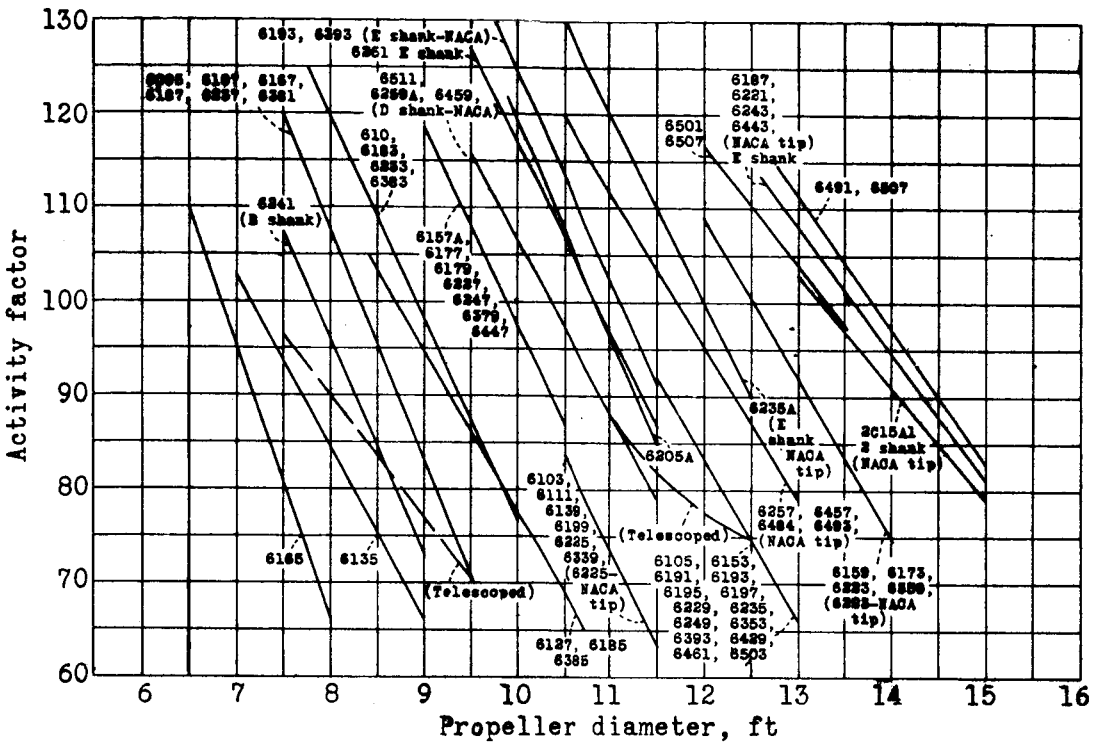

Figure 23.- Activity factors for various Hamilton-Standard propellers. Clark-Y sections except as noted.

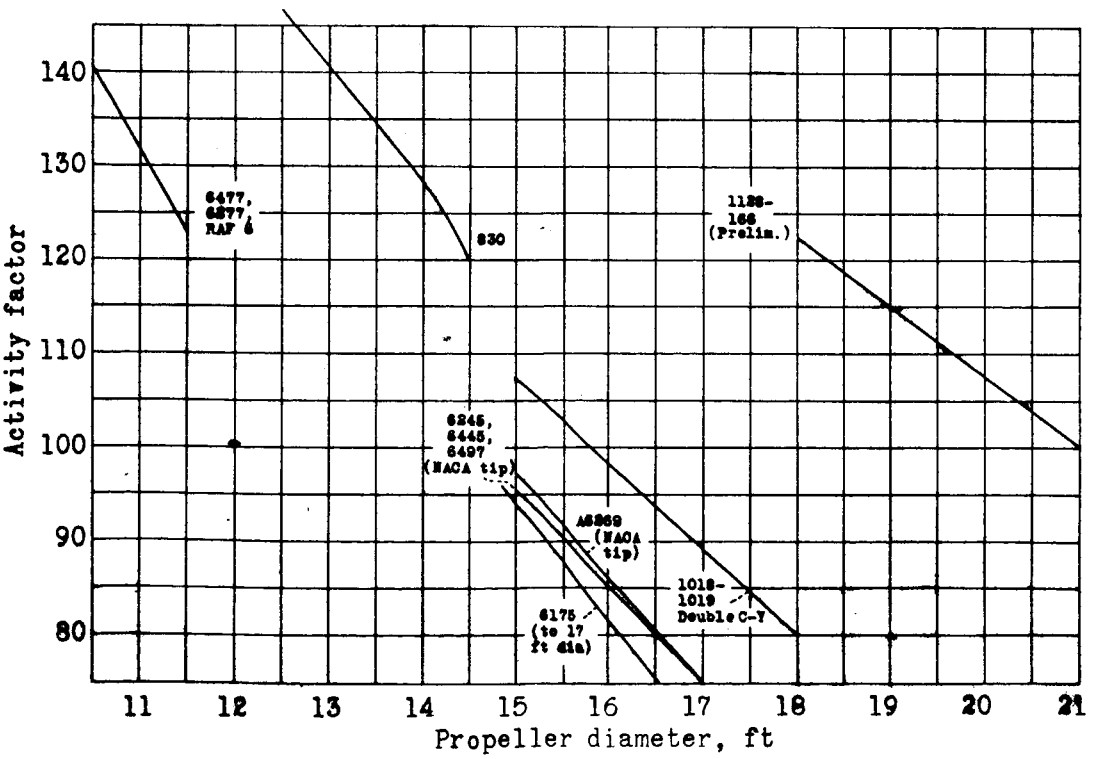

Figure 24.- Activity factors for various propellers.

(1 block = 10/40")